PCP
PLANT & CELL PHYSIOLOGY

Regular Paper

Nitrogen Metabolism is Affected in the Nitrogen-Deficient Rice Mutant *esl4* with a *Calcium-Dependent Protein Kinase* Gene Mutation

Yadi Xing[1,2], Shuang Guo[1,3], Xinlong Chen[1,2], Dan Du[1,2], Mingming Liu[1,2], Yanhua Xiao[1,2], Tianquan Zhang[1,2], Maodi Zhu[1,2], Yingying Zhang[1,2], Xianchun Sang[1,2], Guanghua He[1,2,*] and Nan Wang[1,2,*]

[1]College of Agronomy and Biotechnology, Southwest University, Chongqing 400715, China
[2]Academy of Agricultural Sciences, Southwest University, Chongqing 400715, China
[3]Rice Research Institute, Chongqing Academy of Agricultural Sciences, Chongqing 400715, China
*Corresponding authors: Guanghua He, E-mail, heghswu@163.com; Fax, +86 023 68250158; Nan Wang, E-mail, wangnan_xndx@126.com; Fax, +86 023 68250158.
(Received January 8, 2018; Accepted August 23, 2018)

Calcium-dependent protein kinases are involved in various biological processes, including hormone response, growth and development, abiotic stress response, disease resistance, and nitrogen metabolism. We identified a novel mutant of a calcium-dependent protein-kinase-encoding gene, *esl4*, by performing map cloning. The *esl4* mutant was nitrogen deficient, and expression and enzyme activities of genes related to nitrogen metabolism were down-regulated. *ESL4* was mainly expressed in the vascular bundles of roots, stems, leaves, and sheaths. The ESL4 protein was localized in the cell membranes. Enzyme activity and physiological index analyzes and analysis of the expression of nitrogen metabolism and senescence-related genes indicated that *ESL4* was involved in nitrogen metabolism. *ESL4* overexpression in transgenic homozygous T_2 plants increased nitrogen-use efficiency, improving yields when little nitrogen was available. The seed-set rates, yields per plant, numbers of grains per plant, grain nitrogen content ratios, and total nitrogen content per plant were significantly or very significantly higher for two *ESL4* overexpression lines than for the control plants. These results suggest that *ESL4* may function upstream of nitrogen-metabolism genes. The results will allow *ESL4* to be used to breed novel cultivars for growing in low-nitrogen conditions.

Keywords: Calcium-dependent protein kinase • Early senescence leaf • Efficient nitrogen use • Low nitrogen breeding • Nitrogen metabolism.

Abbreviations: CA, *CARBONIC ANHYDRASE*; CPKs, calcium-dependent protein kinases; GFP, green fluorescent protein; GOGAT, glutamic acid synthase; GS, glutamine synthetase; *GS1*, *GLUTAMINE SYNTHETASE 1*; GUS, β-glucuronidase; N0, ultra-low nitrogen; N1, low nitrogen; N2, standard nitrogen; N3, high nitrogen; *NOL*, *NON-YELLOW COLORING 1 LIKE*; NR, nitrate reductase; ORF, open reading frame; *OsGLN 1; 2*, *GLUTAMINE SYNTHETASE 1; 2*; OsNAPNAC *Family Transcription Factor NAC-LIKE, ACTIVATED BY AP3/PI*; *OsNRT2.2*, *HIGH AFFINITY NITRATE TRANSPORTER 2.2*; *PSR1*, *PROMOTOR OF SHOOT REGENERATION 1*; qRT-PCR, quantitative real-time PCR; *SGR*, *STAYGREEN*; WT, wild-type.

Subject areas: (3) regulation of gene expression, (4) proteins, enzymes and metabolism.

Introduction

Calcium signaling occurs through a highly integrated network and acts as a ubiquitous second messenger, playing important roles in the division, growth, differentiation, aging, apoptosis, and stress resistance of cells (Trewavas and Malhó 1998, Sanders et al. 1999, Berridge et al. 2000). Calcium signal induction is mediated by the activities of many different calcium sensors. Several families of calcium sensors in higher plants have been identified, including calmodulin, calmodulin-associated proteins, calcineurin B-like proteins, and calcium-dependent protein kinases (CPKs) (Roberts and Harmon 1992, Snedden and Fromm 1998, Zielinski 1998, Kudla et al. 1999, Harmon et al. 2000, Kolukisaoglu et al. 2004). These proteins bind to calcium ions, undergo conformational transformations, then transmit the signal to another protein, activating a specific downstream phosphorylation reaction (Harmon et al. 2001, Defalco et al. 2010).

The CPK family of calcium sensors performs several important biological functions in plants. First, CPKs are involved in hormone response. Treating rice seeds with gibberellin (Abo-El-Saad and Wu 1995) and rice leaves with brassinolide (Yang and Komatsu 2000) can increase CPK enzyme activity. Second, CPKs are involved in plant growth and development. Expression of a pollen-specific CPK gene in maize is limited to late pollen development. Applying calmodulin antagonists, CPK inhibitors, and multimeric nucleotide sequences directed against CPK mRNA to cultured pollen inhibits pollen grain germination and pollen tube growth (Estruch et al. 1994). An *OsCPK23* deletion mutant of rice (*Oryza sativa*) has been found to accumulate less starch and protein in the immature seeds than were accumulated in non-mutant seeds (Asano et al. 2002).

Plant Cell Physiol. 59(12): 2512–2525 (2018) doi:10.1093/pcp/pcy169, Advance Access publication on 28 August 2018, available online at www.pcp.oxfordjournals.org

Third, CPKs are involved in abiotic stress responses. Closely related CPKs (AtCPK4 and AtCPK11) have been found actively to regulate abscisic acid signaling pathways and to be involved in seed germination, seedling growth, cytoprotection, and salt tolerance regulation in *Arabidopsis thaliana* (Zhu et al. 2007). The degree to which *OsCPK7* is expressed in rice is closely associated with exposure to cold and to salt and drought stress, and *OsCPK7* overexpression accelerates the response of genes related to salt and drought stress (Saijo et al. 2000). *OsCPK9* positively regulates drought tolerance and spikelet fertility (Wei et al. 2014). Fourth, CPKs are associated with pathogen resistance. *OsCPK4* overexpression in rice significantly enhances salt tolerance, drought tolerance, and rice blast resistance (Campo et al. 2014, Bundó and Coca 2016). Inactivating *NtCDPK2* by virus-induced gene silencing has been found to cause Cf-9-/Avr9-mediated plant hypersensitivity to disappear (Romeis et al. 2000, 2001). CPKs are also involved in carbon and nitrogen metabolism. Sucrose phosphorylase is a key enzyme involved in carbon metabolism. Nitrate reductase (NR) is a rate-limiting enzyme in the nitrogen metabolism process. Phosphorylation of sucrose phosphorylase and nitrate reductase is inhibited in the dark, and CPK-mediated Ca^{2+} signaling is involved in the phosphorylation process (Chung et al. 1999). Sucrose phosphorylase and NR activities in the dark are suppressed by CPK, consistent with the intracellular Ca^{2+} concentration being higher at night than in the day (Johnson et al. 1995). However, CPK may also activate sucrose phosphorylase by phosphorylating Ser424, but this phosphorylation-dependent activation only occurs during hypotonic stress responses (Toroser and Huber 1997).

Nitrogen is an essential nutrient for plants and an important factor limiting crop productivity. Applying nitrogen fertilizer to paddy fields is an important way of improving rice yields. However, applying excess nitrogen fertilizer decreases both the nitrogen absorption efficiency and the efficiency of the fertilizer, and contributes to pollution of the environment with nitrogen. Fully exploiting the genetic potential of rice to make use of nitrogen could allow nitrogen absorption and use by rice to be effectively improved. Nitrogen metabolism by rice is a complex dynamic process involving numerous physiological and biochemical processes, including nitrogen transport, distribution, use, and reuse (Ladha et al. 1998). Nitrogen uptake and use by rice are not independent, but rather form a cyclic metabolic system mediated by a series of enzymes. NR, glutamine synthetase (GS), glutamic acid synthase (GOGAT), and glutamate dehydrogenase are the key enzymes involved in nitrogen metabolism by plants (Marschner 2012). CPKs are also involved in nitrogen metabolism by plants. Calcium signaling mediated by CPK is involved in the phosphorylation of NR, which is accomplished by ser543 phosphorylation and the 14–3-3 protein phosphorylation site in a two-step reaction (Chung et al. 1999). Nitrate–CPK–nin-like protein signaling is key to the nitrogen growth network, nitrogen signal integration and gene expression coordination, nitrogen metabolism, and growth (Liu et al. 2017).

Having previously identified an *esl4* mutant of rice (Guo et al. 2014), in the present study we cloned the *ESL4* gene that encodes a CPK. The active oxygen contents of the leaves were higher and senescence-related genes were expressed more in the mutant than in the wild-type, and the leaves of the mutant senesced prematurely. Nitrogen-metabolism-related gene expression, enzyme activity, and physiological index analyzes indicated that the *esl4* mutant was nitrogen-deficient and that *ESL4* is involved in the nitrogen metabolism process. *ESL4* overexpression improved the nitrogen use efficiency and increased the yield. We investigated the involvement of *ESL4* in nitrogen metabolism regulation and the regulatory gene network. The results presented here improve our understanding of the roles of CPK gene in regulating nitrogen metabolism and provide a molecular basis for elucidating nitrogen uptake mechanisms in plants.

Results

ESL4 encodes a CPK

The early-senescent-leaf rice mutant *esl4* was extracted from ethylmethylsulfonate-induced mutations of 'Jinhui 10' indica rice. The tips and margins of the second, third, and fourth leaves of the *esl4* mutant became yellow in the early tillering stage, and the premature senescence phenotype was developed gradually at an early stage of heading (**Fig. 1A–F**). Transmission electron microscopy images indicated that the chloroplast areas in the mesophyll cells in the apical portions of the leaves were smaller in the mutants than in the wild-type, and the matrix of the mutant chloroplast was blurred and lamellae loose. The photosynthetic pigment contents of the leaves were significantly lower for the mutant than for the wild-type. In a previous study, *ESL4* was localized to a 63 kb region on chromosome 4 (Guo et al. 2014). There are 12 open reading frames in this interval (**Fig. 1G**), and four genes (*LOC_Os04g47240*, *LOC_Os04g47250*, *LOC_Os04g47300*, and *LOC_Os04g47330*) may be associated with plant senescence. The *LOC_Os04g47240* gene encodes an S_TKc protein that belongs to the mitogen-activated protein kinase family, *LOC_Os04g47250* encodes a cytochrome P450 protein, *LOC_Os04g47300* encodes a CPK protein, and *LOC_Os04g47330* encodes a protein associated with rho-GTPase activation. We performed sequence analyzes of the wild-type and *esl4* mutant genomes for each of the four genes. The mutant had a single-base G to A substitution at the 2,511 bp position (522 amino acid glutamic acid) in the last exon of *LOC_Os04g47300* in the genomic DNA (**Fig. 1G** and Supplementary Fig. 1A). However, no difference was found between the mutant and the wild-type cDNA sequences at this site (Supplementary Fig. 1B). These results suggest that RNA editing and repair had corrected the genomic mutation at this site, so the same amino acid was encoded in the mutant and wild-type. Gene and protein expression of *LOC_Os04g47300* in wild-type and *esl4* mutant leaves at the tillering stage were analyzed by western blot analysis and quantitative real-time PCR (qRT-PCR) to determine whether *LOC_Os04g47300* was expressed differently in the *esl4* mutant and wild-type. *LOC_Os04g47300* was expressed significantly less in the *esl4* mutant than in the wild-type (**Fig. 1H and P**). *LOC_Os04g47300* was also expressed less at the protein level in the *esl4* mutant than in the wild-type (**Fig. 1I**). We therefore classed

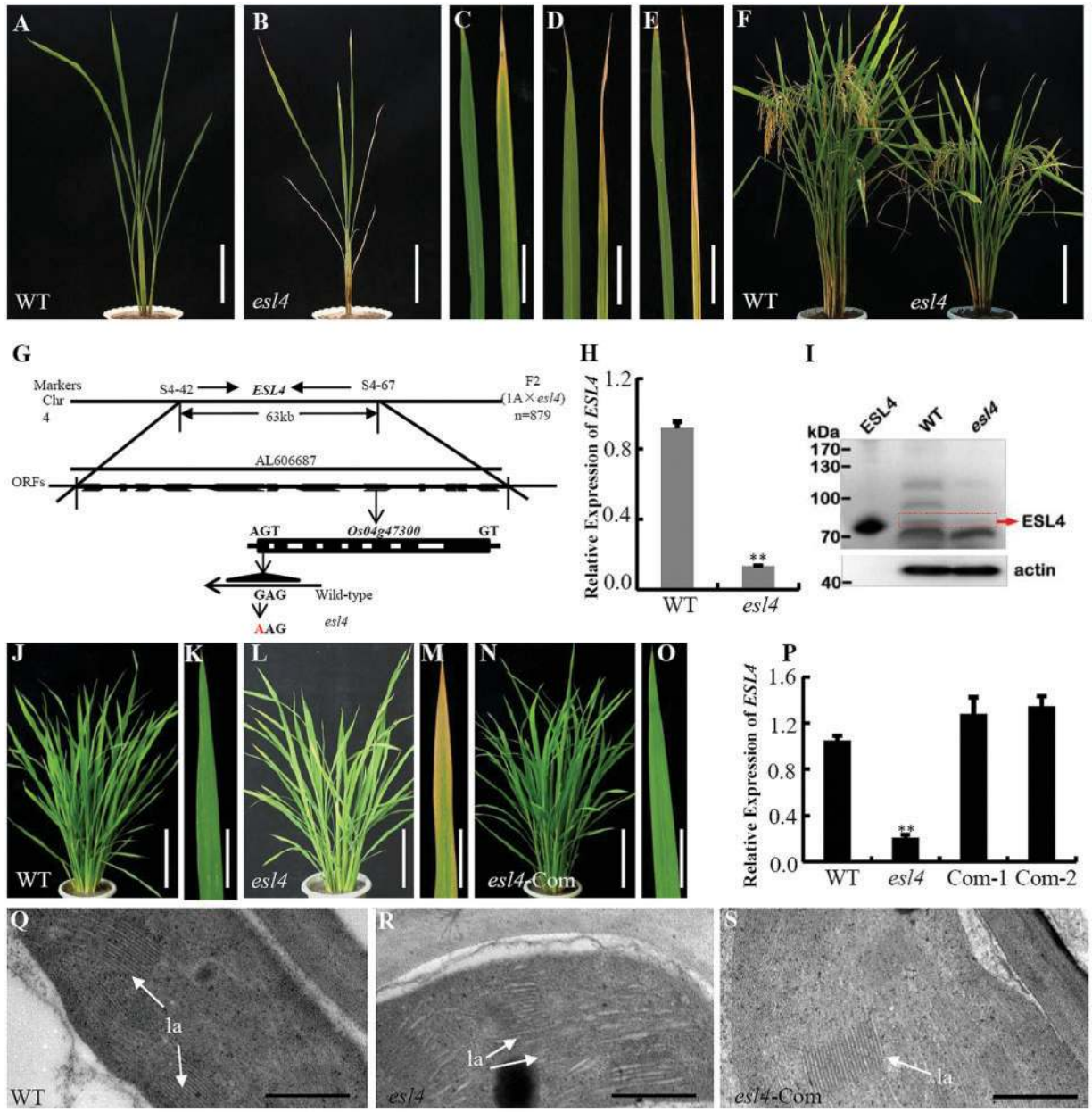

Fig. 1 Results of the phenotypic analysis of the *esl4* mutants and cloning of the *ESL4* gene. (A and B) Morphologies of the wild-type (WT) and *esl4* mutant plants at the early tillering stage. The morphologies of the (C) second, (D) third, and (E) fourth leaves of the WT and *esl4* mutant plants at the early tillering stage are also shown. In each subfigure, the WT is on the left and the *esl4* mutant on the right. (F) Morphologies of the WT and *esl4* mutant plants at the mature stage. (G) Fine mapping of the *esl4* locus on chromosome 4. (I) ESL4 protein expression in the leaves of the WT and *esl4* mutant plants, determined by Western blot analysis. (J–O and Q–S) Phenotypic complementation achieved by introducing *ESL4*. *esl4*-Com means plants transformed with a 8,275 bp WT genomic DNA fragment from *ESL4*. The normal phenotype was recovered in (J, L, and N) plants, (K, M, and O) leaves, and (Q, R, and S) the matrix lamellar structures of the chloroplasts (la, lamella). Bar: (A and B) 15 cm; (C, D, and E) 3 cm; (F, J, L, and N) 20 cm; (K, M, and O) 5 cm; (Q–S) 400 μm. (H and P) Relative expression of *ESL4* in the leaves of the WT and *esl4* mutant plants (H), and in the WT, *esl4* mutant, and two complementary (Com-1 and Com-2) plants (P). The data are shown as the mean ± SD ($n = 3$). An asterisk indicates the mutant was statistically significantly different from the WT (**$P \leq 0.01$).

LOC_Os04g47300 as a candidate gene for *ESL4*. *LOC_Os04g47300* encodes the CPK *OsCPK12*, which is a 2,549 bp single-copy gene, with eight exons and seven introns and encoding 533 amino acids.

We constructed the *LOC_Os04g47300* genome complementary vector, which included the 4,618 bp upstream promoter sequence, coding and noncoding regions, and 1,108 bp downstream 3′ terminal region, then transformed the vector into the *esl4* mutant to determine whether the candidate gene corresponded to *ESL4*. PCR and staining the T_0 generation for β-glucuronidase (GUS) activity indicated that there were 22 positive transformants. No phenotypic differences were found between the 22 transformants and the wild-type throughout

the growth period, and premature senescence was not observed (Fig. 1J–O). We then performed transmission electron microscopy to investigate the structures of the chloroplasts in the leaf tips of wild-type, mutant, and positive complementary plants. The chloroplast areas were larger in the mesophyll cells of the wild-type leaf tips than in the mutant cells, the matrix structure was clear, and the lamellar structure was compact (Fig. 1Q). The chloroplast areas were smaller in the mesophyll cells in the apical portions of the mutant leaves, the matrix structure was blurred, and the lamellae structure was loose (Fig. 1R). The chloroplasts of the positive complementary plants were similar to the chloroplasts of the wild-type plants (Fig. 1S). The chlorophyll and carotenoid contents of the positive complementary plants were not significantly different from the chlorophyll and carotenoid contents of the wild-type plants (Supplementary Fig. 1C). These results demonstrated that *LOC_Os04g47300* was the target gene *ESL4*.

The phylogenetic analysis results indicate that ESL4 belongs to a highly conserved family of CPK proteins and is closely related to OsCPK19 (Supplementary Fig. 2C). It has previously been found that CPK contains an N-terminal variable domain, a kinase catalytic domain, a linker region, and four EF-type domains (Harper et al. 1991, Harmon et al. 2000, Hrabak et al. 2003) (Supplementary Fig. 2A). Multiple amino acid sequence alignments were found for the CPK proteins, indicating that ESL4 has a high sequence similarity with other CPKs (Supplementary Fig. 2B). These results indicate that ESL4 contains typical CPK domains that can bind calcium and participate in signal transduction responses to external signals (Harmon et al. 2000). The *esl4* mutation site was found to be in the fourth EF-type domain of the sixth non-changeable glutamic acid.

Activity analysis of the ESL4 recombinant protein

We performed an in vitro enzyme activity assay to determine whether ESL4 (OsCPK12) has kinase activity. We constructed pet32a vectors to express proteins containing full length ESL4 and truncated ESL4 with truncated C-terminal CaM-like domains in vitro. Expression bands were found in the induced samples but not in the untreated control samples, and the molecular weight was consistent with the expected molecular weight. Full-length ESL4 and truncated ESL4 were successfully expressed (Fig. 2A). The induced cells were purified using a recombinant protein. The purified product was detected by SDS-PAGE, and the high purity recombinant protein was obtained (Fig. 2B). This suggested that the recombinant protein was present as a soluble protein.

The enzyme activity of the recombinant protein was determined using a luminescent kinase assay kit. In the enzymatic reaction catalyzed by full-length ESL4 (Fig. 2C and D), the relative light unit measured in the presence of Ca^{2+} decreased as the reaction time increased, indicating that ATP was continually consumed during the enzymatic reaction and that the full-length ESL4 recombinant protein was catalytically active. Ethylene glycol-bis(β-aminoethyl ether)-N, N, N′, N′-tetraacetic acid is a Ca^{2+}-specific chelating agent that binds to Ca^{2+} during an enzymatic reaction without binding to Mg^{2+}. Adding ethylene glycol-bis(β-aminoethyl ether)-N, N, N′, N′-tetraacetic acid to the solution in the absence of Ca^{2+} did not markedly change the way the luminescence value changed over time, indicating that ESL4 activity was dependent on Ca^{2+}. In the enzymatic reaction catalyzed by truncated ESL4 (Fig. 2E), the luminescence value did not decrease over time even in the presence of Ca^{2+}, indicating that the ATP content of the solution did not change and that the truncated enzyme was not clearly active. These results indicated that ESL4 activity did not respond to Ca^{2+} after the C-terminal CaM-like domain was truncated. In the blank enzymatic reaction (Fig. 2F), the luminescence value did not decrease over time even in the presence of Ca^{2+}, indicating that the ATP content of the solution did not change and no proteins in the solution reacted with Ca^{2+}.

In the enzymatic reaction catalyzed by full-length ESL4, increasing the ESL4 protein concentration caused the relative light unit measurement to decrease, suggesting that the ATP consumption rate of the enzymatic reaction increased. These results indicated that the catalytic activity of the full-length ESL4 recombinant protein was positively correlated with the concentration of the protein (Fig. 2G).

ESL4 is expressed in phloem and localized on cell membranes

We collected root, stem, leaf, sheath, and spike samples at the seedling, tillering, and booting stages, and analyzed the samples using qRT-PCR. *ESL4* was expressed in all of the organs at each developmental stage, so we concluded that it was expressed homogeneously in all tissues (Fig. 3A).

We constructed a P_{ESL4}:: GUS vector and transformed it into wild-type plants. GUS activity staining indicated that *ESL4* was mainly expressed in the root, stem, leaf, and sheath vascular bundles but was also expressed in the spikelet palea and lemma vascular bundles (Fig. 3B–L). We investigated the *ESL4* expression pattern further by performing in situ hybridization, and found that *ESL4* had strong signals in the sheath and stem vascular bundles (Fig. 3M–Q). These results were consistent with the qRT-PCR results, indicating that *ESL4* does not have a tissue-specific expression pattern and is mainly expressed in the vascular bundles of various organs.

We constructed a green fluorescent protein (GFP) fusion vector containing the *ESL4* coding sequence to allow the subcellular localization of the ESL4 protein to be investigated. The vector was transformed into rice protoplasts, and confocal laser microscopy showed that the *ESL4*-GFP fusion protein was localized on the cell membranes (Fig. 4E–H) but the GFP signal was localized in the cytoplasm and nucleus (Fig. 4A–D). These results indicate that ESL4 is a membrane-localized protein.

esl4 is a nitrogen-deficient mutant

Calcium signaling mediated by CPKs is involved in nitrogen metabolism by plants (Chung et al. 1999). Nitrogen metabolism directly affects plant growth during the development stage. We performed transcriptome sequencing of *esl4* and the wild-type, and the differential gene KEGG pathway enrichment results

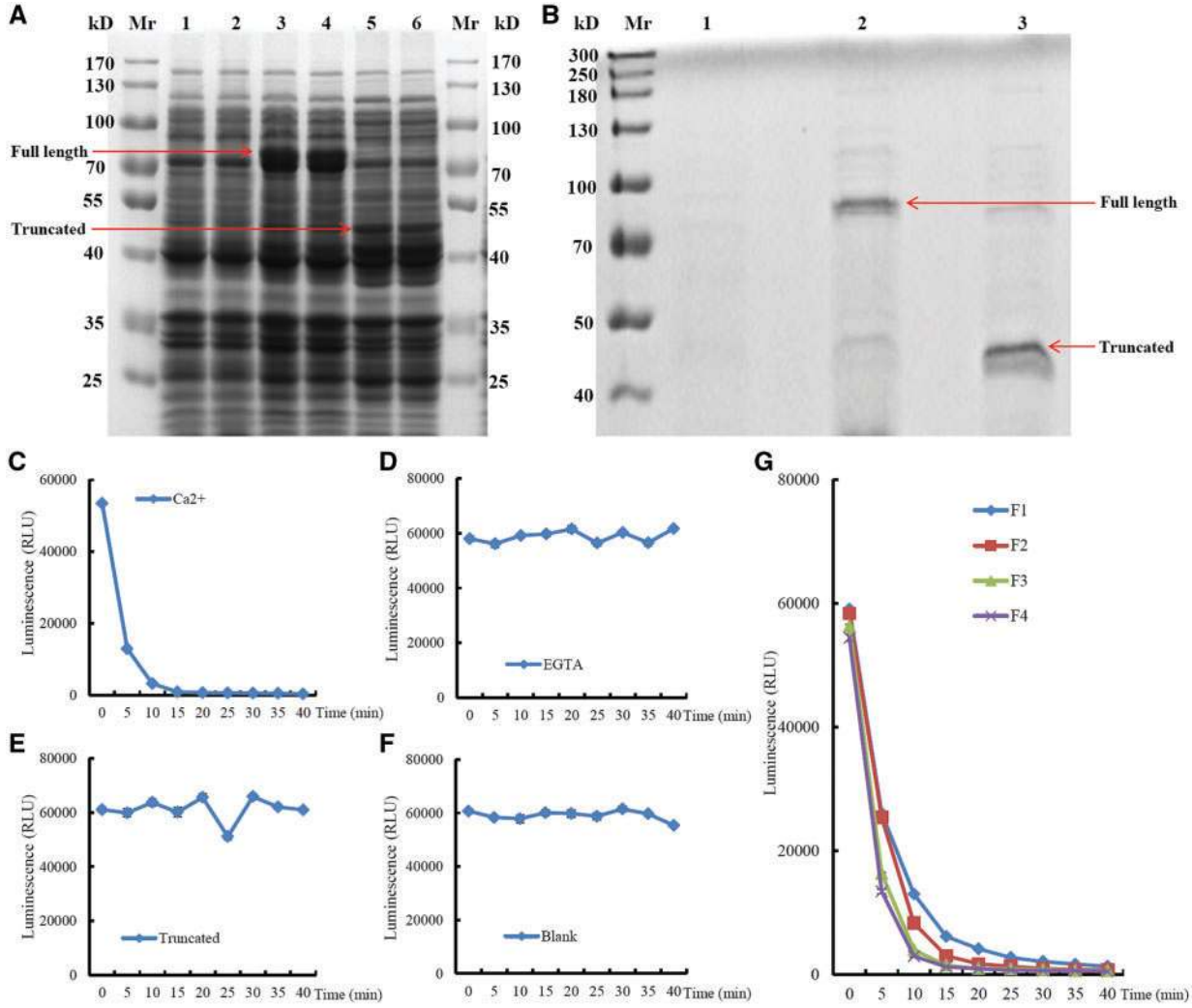

Fig. 2 Expression, purification, and activities of full-length and truncated recombinant ESL4. (A) Expression of full-length and truncated recombinant ESL4. Mr, protein marker; 1–2, induced control; 3–4, induced expression of full-length ESL4; 5–6, induced expression of truncated ESL4. (B) Purification of full-length and truncated recombinant ESL4. 1, purified control; 2, purified full-length ESL4; 3, purified truncated ESL4. (C) Activity of full-length ESL4 in the presence of calcium ions. (D) Activity of full-length ESL4 in the absence of calcium ions. (E) Activity of truncated ESL4 in the presence of calcium ions. (F) Activity of the control in the presence of calcium ions. (G) Activity of full-length ESL4 at different concentrations in the presence of calcium ions. F1, F2, F3, and F4, the reaction was supplemented with 20, 30, 40, and 50 μl, respectively, of purified full-length ESL4 recombinant protein. The data are shown as the mean ± SD (n = 3).

contained four pathways with P values < 0.001 (**Fig. 5A**). Photosynthesis-antenna proteins and photosynthesis pathways were directly related to the premature senescence phenotype but changes in the glyoxylate and dicarboxylate metabolism and nitrogen metabolism pathways were unique to *esl4*. The wild-type and mutant transcriptome sequencing data indicated that one lyoxylate and dicarboxylate metabolism gene and other two senescence-related genes were substantially up-regulated in the mutant (**Fig. 5C**). We quantitatively verified the expression of these aging-related genes, and the results showed that these genes were all up-regulated (data not shown). At the same time, five nitrogen metabolism genes were altered (all were down-regulated) in the mutant (data not shown). The nitrogen metabolism effects of the five genes were quantified, and the different genes were found to be down-regulated to different degrees (**Fig. 5B**). The five genes were *CARBONIC ANHYDRASE* (*CA*), *PSR1* (*PROMOTOR OF SHOOT REGENERATION 1*), *NR*, *OsGLN1; 2* (*GLUTAMINE SYNTHETASE 1; 2*), and *OsNRT2.2* (*HIGH AFFINITY NITRATE TRANSPORTER 2.2*). *OsNRT2.2* encodes a transporter, and the other four genes encode different enzymes involved in the nitrogen metabolism process. An enzyme-linked immunosorbent assay was used to measure the activities of these four enzymes in the wild-type and mutant strains. The results showed that these four enzymes had significantly lower activities in the mutant than the wild-type plants (**Fig. 5D–G**). We therefore hypothesize that the *esl4* mutant phenotype is the result of abnormal nitrogen metabolism. We measured the dry weights, nitrogen content ratios, and total nitrogen contents of wild-type and *esl4* mutant at the tillering, heading, and maturity stages. The dry weights and

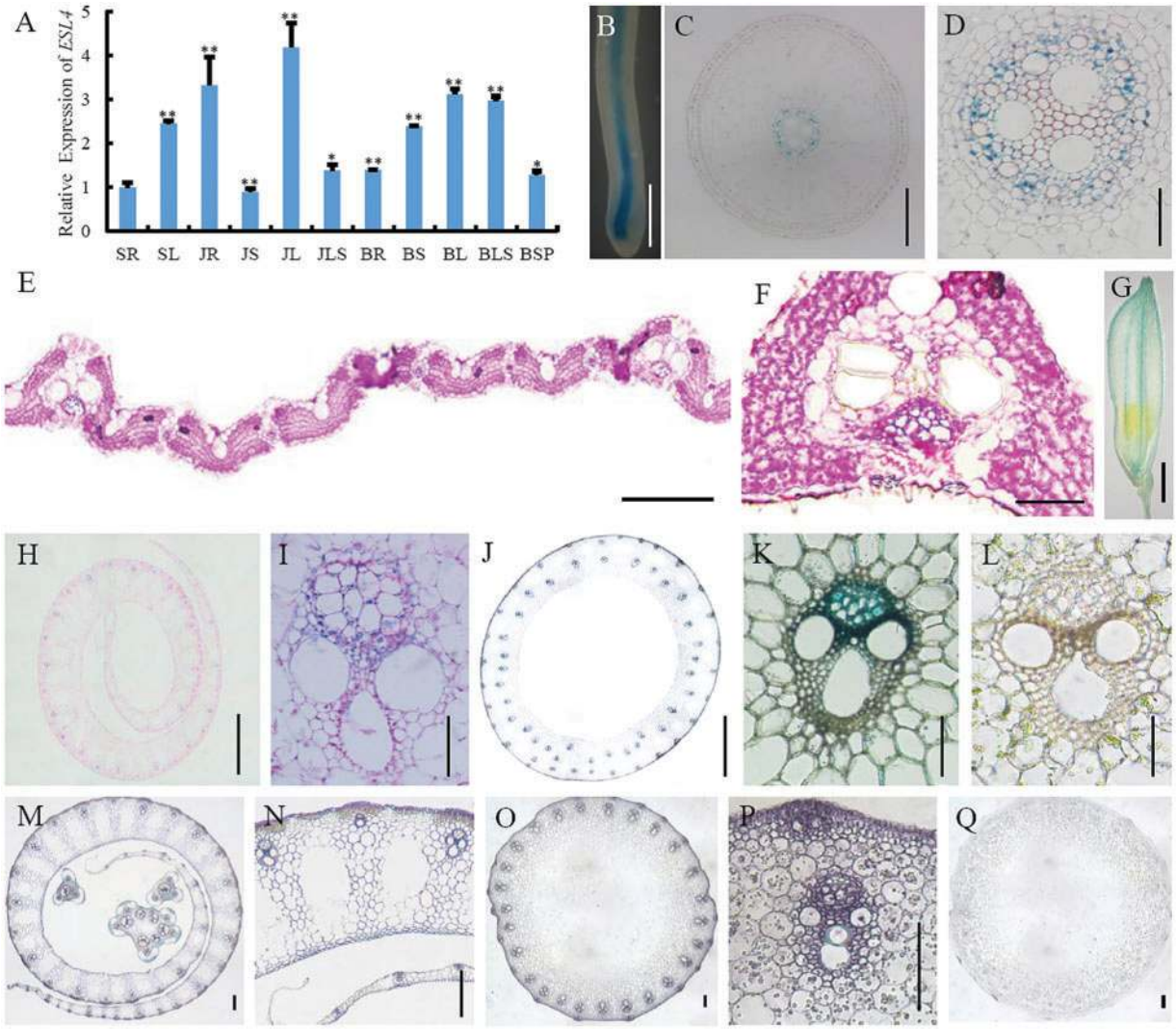

Fig. 3 Expression of *ESL4*. (A) Expression of *ESL4* in various organs of the wild-type plants, analysed by quantitative real-time PCR. SR, seedling stage root; SL, seedling stage leaf; JR, jointing stage root; JS, jointing stage stem; JL, jointing stage leaf; JLS, jointing stage leaf sheath; BR, booting stage root; BS, booting stage stem; BL, booting stage leaf; BLS, booting stage leaf sheath; BSP, booting stage spike 0.5 cm long. The data are shown as the mean ± SD ($n = 3$). An asterisk indicates the test item was statistically significantly different from the SR ($^{*}P \leq 0.05$, $^{**}P \leq 0.01$). (B–L) Histochemical staining for the *ESL4* promoter–GUS reporter gene. The GUS signal was detected in the vascular bundles of the (B–D) root, (E and F) leaf, (H and I) leaf sheath, and (J and K) stem. (G) The GUS signal was detected in the vascular bundles of the spikelets. (L) The GUS signal was not detected in the phloem in the wild-type stem. (M–P) Expression of the *ESL4* gene in the sheaths and stems. A signal was detected in the vascular bundles of the (M and N) sheath and (O and P) stems. (Q) No signal was detected in the stems. Bar: (B, H, and J) 2 mm; (C and F) 100 μm; (D and E) 20 μm; (G) 5 mm; (I, K, and L) 50 μm; (M–Q) 50 μm.

nitrogen content ratios of the leaves and sheaths were significantly lower for the *esl4* mutants than for the wild-type plants at the tillering stage. The leaf and sheath total nitrogen contents were therefore significantly lower for the *esl4* mutants than for the wild-type plants. The dry weights of the vegetative organs and seeds at the heading and maturity stages were significantly lower for the *esl4* mutants than for the wild-type plants, but the nitrogen content ratios and total nitrogen contents of the vegetative organs were significantly higher for the *esl4* mutants than for the wild-type plants and the total nitrogen contents of the seeds were significantly lower for the *esl4* mutants than for the wild-type plants (**Fig. 5H–J**). The nitrogen use efficiency of grain at the maturity stages were significantly lower for the *esl4* mutants than for the wild-type plants (**Fig. 5K**). These results indicated that nitrogen metabolism was defective in the *esl4* mutant.

We determined whether the *esl4* mutant was a nitrogen auxotrophic mutant by exposing plants to four concentrations of exogenous nitrogen (ultra-low nitrogen (N0), low nitrogen (N1), standard nitrogen (N2), and high nitrogen (N3)) in pot experiments (with 0 g (N0), 0.1 g (N1), 0.2 g (N2), and 0.4 g (N3) nitrogen added per kilogram of soil) and field experiments (with 0 g (N0), 90 kg (N1), 180 kg (N2), and 270 kg (N3) nitrogen added per hectare). At the tillering stage, the N1 treatment *esl4* mutant leaf tips prematurely senesced and all the physiological and agronomic traits measured were significantly lower than

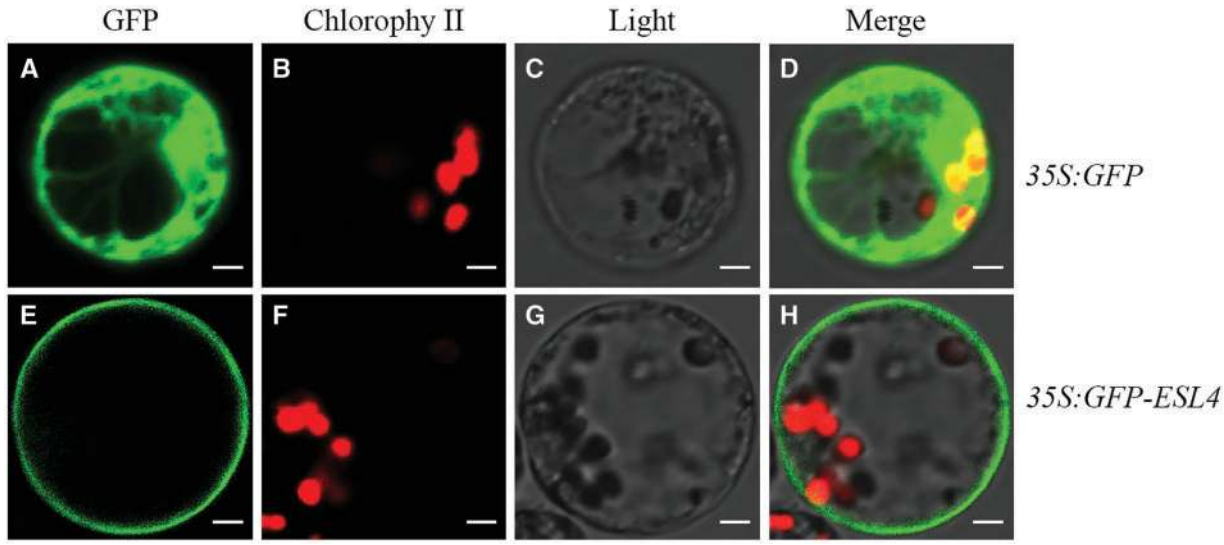

Fig. 4 Subcellular localization of ESL4 fusion protein in rice protoplasts. (A–D) Free GFP was used as a control. (E–H) The ESL4–GFP fusion protein was expressed in rice protoplasts. The GFP fluorescence, chlorophyll autofluorescence, bright-field image, and the merged bright-field, GFP fluorescence, and chlorophyll autofluorescence images are shown. Each scale bar represents 10 μm.

for the wild-type plants. Increasing the amount of nitrogen applied caused senescence to be partially avoided and all the physiological indices of the *esl4* mutants to be partially recovered (**Fig. 6A–H** and Supplementary Fig. 3). The total chlorophyll contents were significantly lower for the mutants than for the wild-type plants, the N0 treatment mutants having only 44.84% of the total chlorophyll contents of the N0 treatment wild-type plants but the N3 treatment mutants having 90.99% of the total chlorophyll contents of the N3 treatment wild-type plants (**Fig. 6I**). The reactive oxygen species contents of the wild-type and *esl4* mutant plants decreased as the amount of nitrogen applied increased, and the difference between the reactive oxygen species contents of the wild-type plants and *esl4* mutants decreased (**Fig. 6J–L**). The N1 treatment wild-type plants grew normally until the maturity period but the *esl4* mutants prematurely aged and the seed-setting rate was lower than for the wild-type plants. Adding exogenous nitrogen caused the agronomic traits of the *esl4* mutants to recover. In particular, the *esl4* mutant seed-setting rate increased from 55.1% of the wild-type seed-setting rate in the N0 treatments to 71.5% of the wild-type seed-setting rate in the N3 treatments (**Fig. 6M**). The *esl4* mutant spike length was significantly lower than the wild-type spike length in the N0 treatments but the *esl4* mutant spike length was not significantly different from the wild-type spike length in the N3 treatments (**Fig. 6N**). The *esl4* mutant yield per plant was 26.07% of the wild-type yields per plant in the N0 treatments but 80.02% of the wild-type yields per plant in the N3 treatments (**Fig. 6O**).

We used qRT-PCR to detect the expression of *ESL4* and genes related to nitrogen metabolism at tillering stages and with different amounts of nitrogen applied. *ESL4* expression in the wild-type increased as the amount of applied nitrogen increased except for the N3 treatment, which had less *ESL4* expression than the N2 treatment. *ESL4* expression in the *esl4* mutant increased as the amount of nitrogen applied increased, from 32.03% of *ESL4* expression in the wild-type in treatment N0 to 115.12% of *ESL4* expression in the wild-type in treatment N3 (Supplementary Fig. 4A). *NR1* and *PSR1* were expressed in the wild-type and *esl4* mutant to a similar degree as *ESL4* was expressed, but unlike in the wild-type, the *NR1* and *PSR1* expression ratio in the *esl4* mutants increased as the amount of nitrogen applied increased (i.e. from the N0 treatment to the N3 treatment) and was almost the same as the ratio for the wild-type plants in the N3 treatments (Supplementary Fig. 4B and C). *CA*, *OsGLN1; 2*, and *OsNRT2.2* expression in the *esl4* mutants did not recover as the amount of nitrogen applied increased (data not shown).

The *esl4* mutants grown under low-nitrogen conditions had premature leaf senescence, but applying nitrogen prevented leaf senescence. We found that the senescence-related genes *NON-YELLOW COLORING 1 LIKE* (*NOL*), *STAYGREEN* (*SGR*), *NAC Family Transcription Factor NAC-LIKE ACTIVATED BY AP3/PI* (*OsNAP*), and *OsL85* were expressed at different tillering stages when different amounts of nitrogen were applied. The degrees to which the senescence-related genes *NOL*, *SGR*, *OsNAP*, and *OsL85* were expressed gradually increased in the wild-type plants but gradually decreased in the *esl4* mutants as the amount of nitrogen applied increased. In the N0 treatments, *NOL*, *SGR*, *OsNAP*, and *OsL85* expression in the *esl4* mutants were 393.86%, 489.87%, 722.68%, and 1,318%, respectively, of the degrees to which they were expressed in the wild-type plants. It can be seen that each gene was expressed markedly more in the mutants than in the wild-type plants. However, increasing the amount of nitrogen applied sharply decreased the expression of these genes in the *esl4* mutants (Supplementary Fig. 4E–G). *NOL* expression changed relatively little, expression in the *esl4* mutants being 393.86%, 239.20%, 109.16%, and 67.72% of expression in the wild-type plants in the N0, N1, N2, and N3 treatments, respectively (Supplementary Fig. 4D).

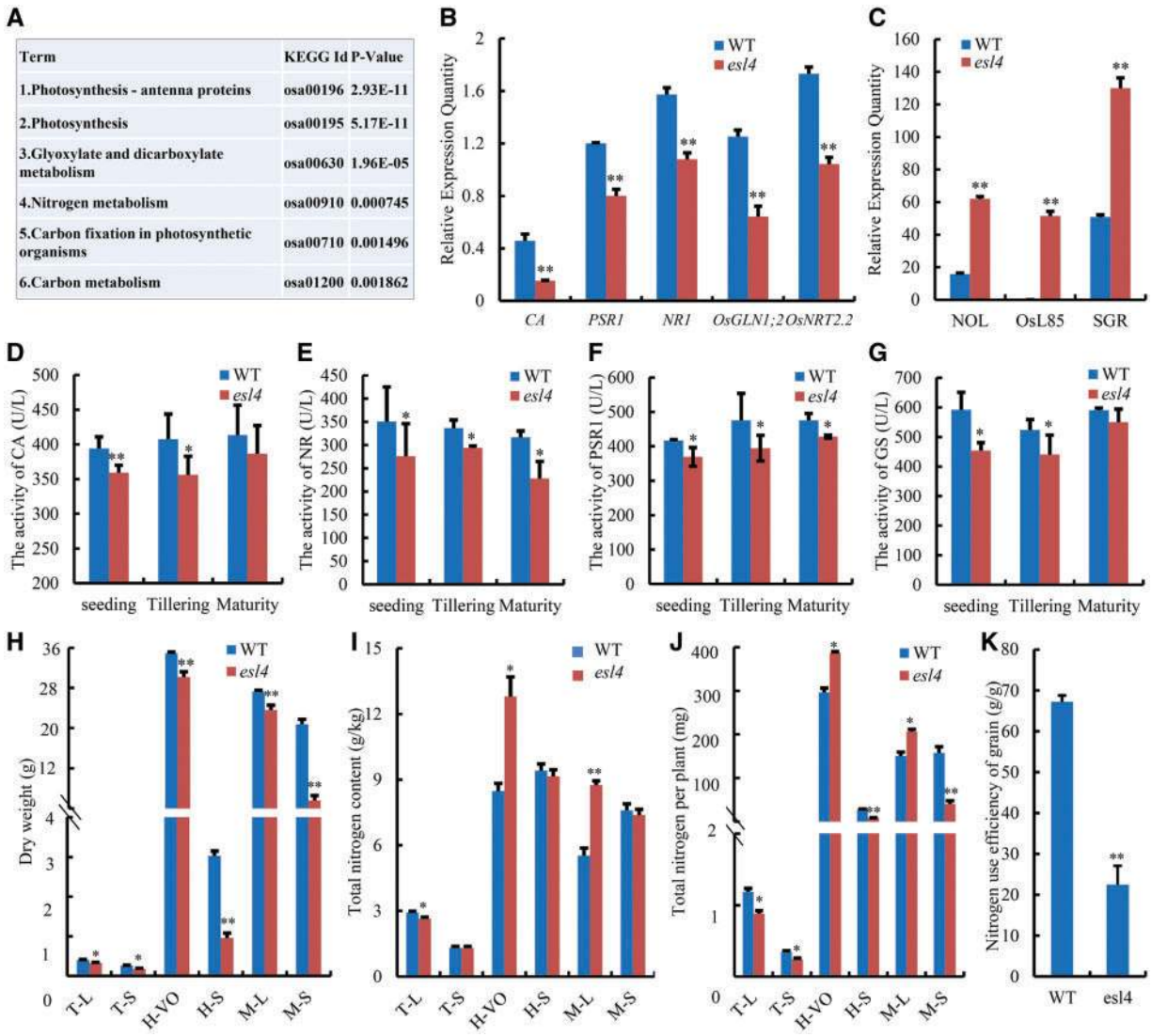

Fig. 5 Expression, enzyme activity, and yield indicator traits for wild-type (WT) and *esl4* mutant plants in the N0 treatments. (A) Differential gene KEGG pathway enrichment in *esl4* and WT transcriptome data. (B) Relative expression of *CA*, *PSR1*, *NR1*, *OsGLN1*; 2, and *OsNRT2.2* in the WT and *esl4* mutant plants in the N0 treatments. (C) Relative expression of *NOL*, *OsL85*, and *SGR* in the WT and *esl4* mutant transcriptome data. (D–G) Activities of (D) CA, (E) NR, (F) PSR1, and (G) GS in the WT and *esl4* mutant plants in the N0 treatments. (H) Dry weights, (I) nitrogen content ratios (g nitrogen per kg weight), (J) total nitrogen contentsper plant, and (K) nitrogen use efficiency of grain for the WT and *esl4* mutant plants in the N0 treatment. T-L, tillering stage leaf; T-S, tillering stage leaf sheath; H-VO, heading stage vegetative organs; H-S, heading stage spike; M-VO, maturity stage vegetative organs; M-S, maturity stage seed. The data are shown as the mean ± SD ($n = 3$). An asterisk indicates that the test item was statistically significantly different from the WT (*$P \leq 0.05$, **$P \leq 0.01$).

Overexpression of *ESL4* increased the total yield under low-nitrogen conditions

We constructed an *ESL4* overexpression vector and obtained positive homozygous T_2 transgenic lines using the *Agrobacterium tumefaciens* infection technique (**Fig. 7A–F**). We selected two T_2 transgenic lines (OE-3 and OE-4) that expressed *ESL4* relatively strongly (**Fig. 7G**) and the trans-loaded control, and cultivated the plants in a field trial using the N0, N1, and N2 nitrogen applications described earlier. The seed-setting rates, yields per plant, numbers of grains per plant, grain nitrogen content ratios, and total nitrogen contents of the seeds per plant were significantly or highly significantly higher in the overexpressed plants than in the controls (**Fig. 7H–L**). In particular, the yields per plant were 14.34% and 20.41% higher for the OE-3 and OE-4 plants, respectively, than for the controls in the N0 treatments and 3.45% and 13.21% higher for the OE-3 and OE-4 plants, respectively, than for the control in the N1 treatments (**Fig. 7I**). The total nitrogen contents per plant were 21.69% and 26.96% higher for the OE-3 and OE-4 plants, respectively, than for the controls in the N0 treatments and 8.73% and 20.28% higher for the OE-3 and OE-4 plants, respectively, than for the controls in the N1 treatments (**Fig. 7L**). The nitrogen use efficiency of grain at the maturity stages was higher in the overexpressed plants than in the controls (**Fig. 7M**). No significant differences were found in the yield indicator traits for the overexpression lines and the controls in the N2 treatments (data not shown).

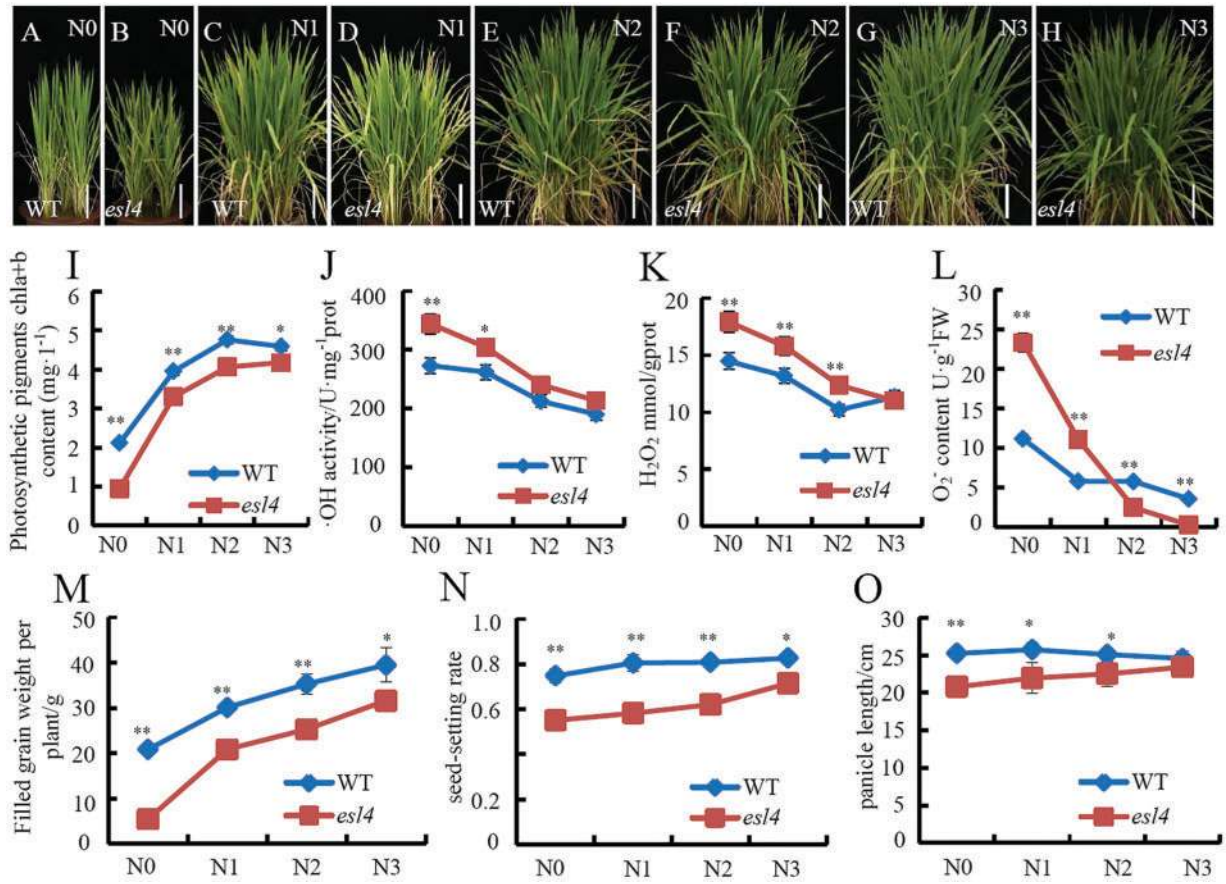

Fig. 6 Phenotype and physiological and biochemical characteristics of wild-type (WT) and *esl4* mutant plants grown with different nitrogen application rates. (A–H) Morphologies of the WT and *esl4* mutant plants after applying nitrogen at the booting stage (applied 70 d after transplanting). Each scale bar represents 20 cm. (I) Photosynthetic pigment (chlorophyll *a* and *b*) contents, (J) •OH activities, (K) H_2O_2 contents, (L) O_2^- contents, (M) filled grain weights per plant, (N) seed-setting rates, (O) panicle lengths of the WT and *esl4* mutant plants in the N0 to N3 treatments. Each error bar indicates the SD ($n = 9$ individual plants). An asterisk indicates the test item was statistically significantly different from the WT ($^*P \leq 0.05$, $^{**}P \leq 0.01$).

The two overexpression lines expressed *ESL4* significantly more than the controls in the N0 and N1 treatments (Supplementary Fig. 5A). *NR1*, *PSR1*, *CA*, *OsGLN1; 2*, and *OsNRT2.2* were up-regulated in the overexpression lines relative to the controls to different degrees in the N0 and N1 treatments (Supplementary Fig. 5B–F). *NOL*, *SGR*, and *OsNAP* were expressed slightly less in the overexpression lines than in the controls (Supplementary Fig. 5G–5I). *OsL85* expression was significantly down-regulated in the overexpression lines relative to the controls, expression in the OE-3 and OE-4 plants being 6.80% and 17.42%, respectively, of expression in the controls in the N0 treatments and 28.25% and 57.88%, respectively, of expression in the controls in the N1 treatments (Supplementary Fig. 5J).

Discussion

ESL4 encodes a CPK, and a mutation of *ESL4* resulted in a new mutant

Calcium-dependent protein kinase cDNA was first isolated from *Arabidopsis*, and CPK genes have since been cloned from various plant species, including carrots, maize, mung beans, rice, and tobacco (Harper et al. 1991). CPKs perform numerous biological functions, participating in hormone responses (Abo-El-Saad and Wu 1995, Sheen 1996, Yang and Komatsu 2000), regulating growth and development (Estruch et al. 1994, Hepler et al. 2001), mediating abiotic stress signal transmission (Bush 1995, Trewavas 1999, Knight and Knight 2001), being involved in resistance to pathogens (Xu and Heath 1998, Blume et al. 2000, Fellbrich et al. 2000, Grant and Loake 2000, and participating in carbon and nitrogen metabolism (Johnson et al. 1995, Chung et al. 1999, Liu et al. 2017). In this study we identified the nitrogen-deficient rice mutant *esl4*. Genome and cDNA sequencing analyses showed that the *ESL4* gene in the *esl4* mutant had a G-to-A single-base mutation at position 2,511 in the last exon, which significantly decreased the amount of *ESL4* RNA and protein in the *esl4* mutant. The EF-type domain structure consists of 12 amino acid residues, with glutamic acid always being at position 6 to ensure that the protein structure is stable (Luan et al. 2002). The bases at positions 2,511–2,513 in the *ESL4* coding region therefore encode a glutamate residue, the most important core amino acid for maintaining the CPK hand-shaped domain. Mutation of this residue would affect the stability of the CPK, resulting in the

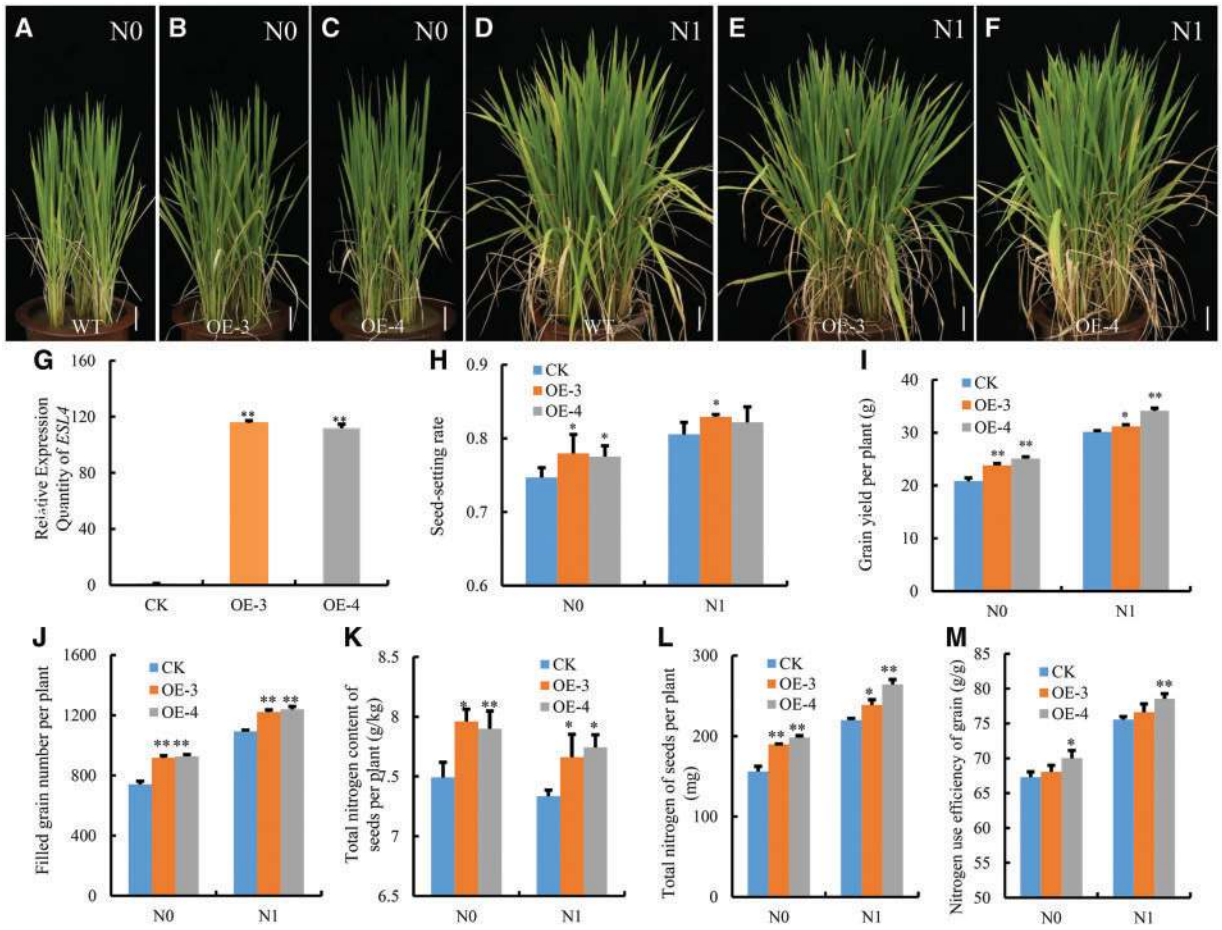

Fig. 7 Phenotypes and characteristics of transgenic plants that overexpressed *ESL4* grown under ultra-low-nitrogen and low-nitrogen conditions. (A–F) Morphologies of the control check (CK) and two transgenic lines (OE-3 and OE-4) that overexpressed *ESL4* after applying nitrogen at the booting stage (applied 70 d after transplanting). Each scale bar represents 10 cm. (G) Relative expression of *ESL4* in the CK and two transgenic lines (OE-3 and OE-4) that overexpressed *ESL4*. (H–L) Statistical data for the (H) seed-setting rates, (I) grain yields per plant, (J) filled grain numbers per plant, (K) total nitrogen contents of the seeds, (L) total nitrogen contents of the seeds per plant and (M) nitrogen use efficiency of grain for the control and two transgenic lines. Each error bar indicates the SD ($n = 30$ individual plants). An asterisk indicates that the test item was statistically significantly different from the control ($^*P \leq 0.05$, $^{**}P \leq 0.01$).

fourth-hand structure of the CPK failing to combine with Ca^{2+} and therefore being dysfunctional. RNA editing repair may have occurred at this site in the *esl4* mutant after the genome mutation had occurred to regain the stability of the EF structure. The amino acid and protein in the *esl4* mutant and the wild-type were identical, but *ESL4* and protein were expressed significantly less in the *esl4* mutant than in the wild-type. It has been predicted, using PREP-mt software with a cutoff of 0.6, that 1,084 sites in the *Cycas* mtDNA protein coding gene are C→U RNA editing sites (Mower 2005). This is typical of RNA replacement (modification), which includes C→U (Chen et al. 1990, Wang et al. 2004), A→I (Yang et al. 2008), A→G (Petschek et al. 1996), and U→C (Chaw et al. 2008) RNA editing. RNA editing sites can support racial development through genetic variation (Yang et al. 2008) and repair harmful genomic mutations (Gray and Covello 1993).

We constructed full-length and truncated ESL4 recombinant proteins to investigate the role of the C-terminal CaM-like domain in the CPK protein. Activity analysis indicated that ESL4 activity was calcium-dependent and that the activity of the truncated protein without the C-terminal CaM-like domain was inhibited and no longer stimulated by Ca^{2+}. This suggests that the CaM-like domain activates CPKs by binding Ca^{2+}, consistent with the CPK protein family regulation mechanism. The protein sequence in the *esl4* mutant was the same as the protein sequence in the wild-type, but *ESL4* was expressed significantly less in the *esl4* mutant than in the wild-type, which could have caused the ESL4 protein concentration to be lower in the *esl4* mutant than in the wild-type. The catalytic activity of the full-length ESL4 recombinant protein in the presence of Ca^{2+} was positively correlated with the ESL4 concentration. The lower ESL4 protein concentration in the *esl4* mutant means the ESL4 catalytic activity is lower than in the wild-type, and this may be why the *esl4* mutant has a mutant phenotype.

ESL4 may be involved in regulating nitrogen metabolism

Following transcriptome sequencing and quantitative verification, we found that expression of five important genes involved in nitrogen metabolism was down-regulated in the mutant compared with the wild-type. *OsNRT2.2* was found to encode

a transporter, and the other four genes were found to encode different enzymes involved in nitrogen metabolism. The activities of these four enzymes were significantly lower in the *esl4* mutant than in the wild-type, indicating that nitrogen metabolism was defective in the mutant. The ability of a plant to take up nitrogen and maintain nitrogen balance is an important factor in the normal development of the plant. In the experiments with different amounts of nitrogen fertilizer added, we found that the *esl4* mutant was sensitive to exogenous nitrogen and that increasing the amount of nitrogen applied improved the ability of the mutant phenotype to avoid premature leaf senescence, indicating that the *esl4* mutant was nitrogen deficient.

Endogenous nitrogen is translocated as amino acids through the roots and above-ground organs. Nitrogen absorbed by the roots is transported in the xylem to the above-ground organs, and a portion of the nitrogen is retransported through the phloem to the roots as a signal to regulate nitrogen absorption by the roots (Larsson et al. 1991). The GUS test and in situ hybridization test results indicated that *ESL4* was expressed in the vascular bundles of various organs. Some other CPKs had similar expression patterns. *OsCDPK19* was expressed more in the vascular tissues of leaves and stems than in other tissues, suggesting that these tissues contain regulatory elements that control expression of the downstream genes (Wang et al. 2007). Phloem is an important source-to-sink transfer route for nitrates involved in the nitrogen metabolism pathway (Fan et al. 2009). We found that the nitrogen contents of vegetative organs such as stems and leaves were significantly higher for the *esl4* mutant than for the wild-type but that the nitrogen content of the grain was significantly lower for the *esl4* mutant than for the wild-type, indicating that nitrogen was transported to the grain in the *esl4* mutant relatively inefficiently. Consistent with this interpretation, the expression analysis results suggested that *ESL4* may be involved in the regulation of nitrogen transport.

Plants decompose and recycle nutrients in ageing organs and initiate senescence-related genes expression to maintain metabolic balance. Nutrients are transferred from senescent organs to reproductive organs or actively growing organs to allow the nutrients to be fully used, meaning that ageing and senescence are necessary for normal plant growth and development (Lim et al. 2007). The *SGR* gene encodes the chloroplast transport peptide protein, and its overexpression can decrease the lamellar structures of thylakoids, leading to leaf yellowing. *NOL* encodes chlorophyll *b* reductase, and a mutation gives a stay-green phenotype. *OsNAP* overexpression accelerates leaf senescence (Jiang et al. 2007, Park et al. 2007, Sato et al. 2009, Zhou et al. 2013). *SGR*, *NOL*, and *OsNAP* were expressed markedly more in the *esl4* mutant than in the wild-type, especially under N0 conditions. This reflects the fact that the needs of the plant are not met in a low-nitrogen environment, meaning that the plant up-regulates chloroplast-degradation-related gene expression in aged leaves to release nitrogen. *OsL85* encodes isocitrate lyase (which is involved in fatty acid metabolism), which is the key rate-limiting enzyme in the glyoxylic acid cycle. *OsL85* is a senescence-related gene, and involved in fatty acid degradation and remobilization (Lee et al. 2001). *OsL85* was expressed markedly more in the *esl4* mutant than in the wild-type, indicating that more fatty acid was degraded and remobilized in *esl4* mutant (Lee et al. 2001).

Overexpression of *ESL4* increases nitrogen-use efficiency under low-nitrogen conditions

Future breeding developments will focus on green, mechanized, and high-quality approaches. The pressure to achieve environmental sustainability means that a key aim for crop breeders is to increase food production under low-nitrogen conditions. It is therefore very important to study the effects of decreasing nitrogen fertilizer application rates and to improve the efficiency with which nitrogen is used by crops to reduce pollution and ensure continued increases in rice yields. *GLUTAMINE SYNTHETASE 1* (*GS1*) overexpression in rice improves nitrogen-use efficiency (Brauer et al. 2011). Plant biomass and leaf-protein content are higher in tobacco plants that overexpress the *GS1* gene than in plants that do not, indicating that *GS1* may improve nitrogen-use efficiency in transgenic plants (Oliveira et al. 2002). *GOGAT* overexpression in transgenic plants can improve nitrogen-use efficiency, and *OsNADH-GOGAT1* overexpression in rice has been found to increase spike weight by 80% (Yamaya et al. 2002). *OsARG* overexpression in rice has also been found to increase nitrogen-use efficiency (Ma et al. 2013). Introducing indica rice type *NRT1.1B* into japonica rice has been found to increase yield and nitrogen-use efficiency, indicating that *NRT1.1B* could improve nitrogen-use efficiency in japonica rice (Hu et al. 2015).

It has been found that *ESL4* (*OsCPK12*) promotes salt tolerance, negatively regulates disease resistance, and may be involved in the abscisic acid signalling pathway (Asano et al. 2012). *OsCPK12* overexpression in incubator-grown plants increased the dry weights of shoots and the total nitrogen contents of the plants (Asano et al. 2010). We used rice mutants in which the CPK gene *ESL4* was overexpressed, driven by the *Cauliflower mosaic virus* 35S promoter. In studies in the field and in pots, the yields per plant, numbers of grains per plant, seed-setting rates and total nitrogen contents were significantly higher for the overexpression plants than for the controls. The higher rice yields and nitrogen use efficiency of grain for the overexpression lines than for the controls were especially marked under ultra-low-nitrogen and low-nitrogen conditions. *ESL4* is not only involved in nitrogen metabolism but is also directly involved in controlling the rice yield, meaning the function of *ESL4* and its role in regulating nitrogen metabolism should be analyzed further.

Materials and Methods

Plant materials and growth conditions

The early senescent rice mutant *esl4* was previously derived from ethyl-methylsulfonate-induced mutagenesis of 'Jinhui 10' indica rice. The *ESL4* gene was localized to a 63 kb region on chromosome 4 (Guo et al. 2014).

All plants were grown at an experimental farm run by the Rice Research Institute of the College of Agronomy and Biotechnology, Southwest University, Chongqing, China. Each plant was grown in soil, either in the field or in a pot.

The total nitrogen, total phosphorus, and total potassium contents of the soil were 0.97, 0.67, and 19.18 g/kg, respectively. The available phosphorus and available potassium contents of the soil were 40 and 225 mg/kg, respectively. Nitrogen fertilizer was applied to the pots using four application rates, 0, 0.1, 0.2, and 0.4 g per kilogram of soil for the N0, N1, N2, and N3 treatment pots, respectively. Nitrogen fertilizer was also applied in the field experiment at four application rates, ultra-low nitrogen (0 kg/ha; N0), low nitrogen (90 kg/ha; N1), standard nitrogen (180 kg/ha; N2), and high nitrogen (270 kg/ha; N3). During the growth period of an experiment, 40% of the nitrogen fertilizer was applied as a base application three days before the plants were transplanted, 30% was applied at the tillering stage (20 d after transplanting), and 30% was applied at the booting stage (70 d after transplanting). A standard fertilizer was applied to the pots, giving P_2O_5 and K_2O application rates of 0.1 and 0.2 g per kilogram of soil, respectively, and a base fertilizer was applied to the field plots in a single dose to give P_2O_5 and K_2O application rates of 100 and 120 kg/ha, respectively. The nitrogen fertilizer was urea (46.4% N), the phosphate fertilizer was superphosphate (containing 12% P_2O_5), and the potassium fertilizer was potassium chloride (containing 60% K_2O). The rice growth period was divided into five stages, namely seedling, tillering, jointing, heading, and maturity.

Gene cloning and sequence analysis

The candidate genes were amplified from the *esl4* mutant and wild-type 'Jinhui 10' DNA and cDNA. Specific primers were designed from the DNA and cDNA sequences of Nipponbare japonica rice (http://www.gramene.org/). The amplified PCR product was recovered using a DNA gel recovery kit (Beijing Tian Gen Biochemical Co., Beijing, China), then inserted into the vector pMD19-T (Takara Bio Inc., Dalian, China) and transformed into *Escherichia coli* strain DH5α. Positive colonies were sequenced by Shanghai Invitrogen Biotechnology Co. (Shanghai, China). The sequences were compared using Vector NTI Advance 10 (Invitrogen; http://www.invitrogen.com/). All the primers used are shown in Supplementary Table 1 (available online).

Vector construction for genetic complementation and Pro_{ESL4}:: GUS

Complementation of the *esl4* mutant was achieved by amplifying a 8,275 bp genomic DNA fragment containing the entire 2,549 bp *ESL4* coding and non-coding regions, a 4,618 bp upstream region, and a 1,108 bp downstream region from the 'Jinhui10' genomic DNA, and the amplified fragments were cloned into the pCA1301 vector.

The Pro_{ESL4}:: GUS vector was constructed by amplifying the upstream 4,618 bp promoter sequence of *ESL4* from the 'Jinhui 10' genomic DNA, then cloning the sequence into the pCA1301 vector.

Full-length and truncated ESL4 prokaryotic expression and purification of recombinant proteins

A pet32a vector containing full-length ESL4 and another containing truncated ESL4 without the C-terminal CaM-like domain were constructed. The full-length and truncated recombinants were transformed into *E. coli* induced using isopropyl β-D-thiogalactoside. The cells were collected and analysed by SDS-PAGE along with untreated control cells.

The induced cells were cleaved by applying ultrasound, then the mixture was centrifuged at a high speed, and the recombinant protein in the supernatant was purified. The recombinant protein ended with a 6X His purified tag, allowing the protein to be purified using a Beaver Beads™ IDA-Nickel kit (cat no. 70501-klo; Haitian Nano Technology Co., Suzhou, China).

Determining the activities of full-length and truncated ESL4 kinase

Recombinant full-length and truncated ESL4 enzyme activity assays were performed using a Kinase-Glo® Luminescent Kinase Assay kit (cat no. #V6071; Promega Biotechnology Co., Beijing, China). Enzymatic buffer and Syntide2 substrate were added to an electrophoresis tube. Recombinant proteins were added to start the reaction, and the reaction mixture was transferred to a white 96-well reaction plate when the reaction stopped. Luminescence was measured as specified in the Kinase-Glo® Luminescent Kinase Assay kit instructions.

Expression analysis

Total RNA was extracted from various tissues using a Total RNA Extraction and Purification kit (Tiangen Biochemical Technology Co., Beijing, China). First-strand cDNA was synthesized using an UEIris RT Reagent kit (US Everbright Inc., Suzhou, China). qRT-PCR was performed using an ABI Prism 7500 Real-Time PCR system (Invitrogen) using a NovoStart® SYBR SuperMix Plus kit (Novoprotein Technology Co., Shanghai, China). Relative expression of each gene was calculated using the $2^{-\Delta\Delta Ct}$ method and expressed relative to *OsActin* expression.

In situ hybridization

The 484 bp gene-specific ESL4 probe was amplified using the Prob-*ESL4*-F and Prob-*ESL4*-R primers and labeled using a DIG RNA labeling kit (SP6/T7; Roche, Germany) following the manufacturer's instructions. Section pretreatment, hybridization, and immunological detection were performed using previously described methods (Sang et al. 2012). The primer pairs used are shown in Supplementary Table 1.

Determining enzyme activity

Fresh plant tissue was thoroughly ground in liquid nitrogen and extracted with 0.1 mM phosphate-buffered saline at pH 7.4 (using a fresh sample weight: extractant volume ratio of 9) at 4°C for 2 h. The sample was then centrifuged at 3,000 rpm for 10 min at 4°C, and the enzyme activity in the supernatant was determined. The enzyme activity was determined using plant CA, NR, PSR1, GS ELISA test kits following manufacturers' instructions.

Western blot analysis

Each harvested sample was mixed with a grinding buffer (containing 50 mM Tris, 150 mM NaCl, 10 mM $MgCl_2$, 0.1% NP-40, and 1 mM phenylmethanesulfonyl fluoride at pH 7.5). The buffer was prepared by dissolving one complete protease inhibitor EASYpack tablet (Roche) in 10 mL of lysis buffer. The lysate samples were immediately denatured at 100°C for 10 min, then sonicated, and then diluted by a factor of three with loading buffer (containing 187.5 mmol/L Tris-HCl, 6% sodium dodecyl sulfate, 30% glycerol, 150 mmol/L DL-dithiothreitol, and 0.3% bromphenol blue at pH 6.8), and the mixture was heated to 100°C for 5 min. The protein extracts were then separated by SDS-PAGE using a 4%–15% polyacrylamide system. The resolved proteins were transferred to polyvinylidene fluoride membranes, blocked by incubating the membranes with 5% non-fat milk for 1 h, and then the membranes were incubated at 4°C overnight with ESL4 primary antibodies.

Transcriptome analysis

The second leaf was collected at the tillering stage. The RNA was extracted and subjected to transcriptome sequencing. Each sample was analysed in duplicate. The RNA purity and concentration were determined using a NanoPhotometer spectrophotometer (Implen, Westlake Village, CA, USA) and a Qubit RNA Assay kit and a Qubit 2.0 fluorometer (Life Technologies, Carlsbad, CA, USA). A library was constructed and RNA sequencing performed by Novogene Bioinformatics Institute (Beijing, China) using a HiSeq 4000 system (Illumina, San Diego, CA, USA). Differentially expressed genes were identified using the DESeq R software package, and the P values were adjusted using the Benjamini and Hochberg approach to control the false discovery rate. Differentially expressed genes with adjusted P values <0.05 were used in the gene ontology enrichment analysis using the AgriGo system (http://bioinfo.cau.edu.cn/agriGO/).

ESL4 structure and sequence analysis

Amino acid sequences for the plant ESL4 proteins were aligned using Vector NTI Advance 10 software. Proteins homologous to ESL4 were obtained from the US National Center for Biotechnology Information (http://www.ncbi.nlm.nih.gov/), Phytozome 10.3 (http://phytozome.jgi.doe.gov/pz/portal.html), and UniProt (www.uniprot.org/) databases. A neighbor-joining tree was

constructed using MEGA v6.0 software, and support for the tree topology was obtained using the bootstrap method with 1,000 replicates (Tamura et al. 2013).

Subcellular localization

The full-length coding sequence of *ESL4* was fused to the N-terminus of GFP controlled by the *Cauliflower mosaic virus* 35S promoter at the *Xho*I and *Spe*I sites of the pA7-GFP vector, giving a pESL4-GFP construct. pESL4-GFP and the empty pA7-GFP vectors were transformed into rice protoplasts (Chen et al. 2006). GFP fluorescence was determined using an LSM710 confocal laser scanning microscope (Zeiss, Jena, Germany).

Determining the total nitrogen content

Each dried whole plant tissue sample was mixed thoroughly, and the total nitrogen content was determined using a KDY-9830 Kjeldahl system (RuiBangXingYe, Beijing, China, http://www.rbxycn.com/) following a previously described method (Fan et al. 2007).

Statistical evaluation

We used four nitrogen application rates in the field experiment. Wild-type, mutant, and two over-expressing strains (OE-3 and OE-4) were arranged in random blocks, with a conservation line around each block. Each treatment was performed in three replicate blocks. In each block, 100 plants were planted in 10 rows. Statistical analyses of the gene expression, chlorophyll content, active oxygen content, and enzyme activity data required six samples from each set of triplicate plots to be analysed, with paired samples from individual plots being analysed independently. Each experiment was performed three times, and there were nine biological replicate experiments. Statistical analysis of the agronomic traits required 10 samples to be collected from each of the three replicates of each community, with a total of three biological replicates. Statistical analysis of the dry weight and nitrogen content measurements indicated that three replicate plots for each treatment were required. Ten samples were taken from each plot, and a total of three biological replicates were performed.

Supplementary Data

Supplementary data are available at PCP online.

Funding

This work was supported by the National Natural Science Foundation of China (grant no. 31371597), the Ministry of Science and Technology major research and development programme (grant no. 2017YFD0100201), the Chongqing Municipal Science and Technology Commission theme special programme (grant nos. cstc2016shms and ztzx0017), the Ministry of Agriculture public welfare industry special programme (grant no. 201303129), the Chongqing Graduate Scientific Research Innovation Project (grant no. CYB14048), and a Chongqing Municipal Science and Technology Commission Project (grant no. CSTCCXLJRC201713).

Disclosures

The authors have no conflicts of interest to declare.

References

Abo-El-Saad, M. and Wu, R. (1995) A rice membrane calcium-dependent protein kinase is induced by gibberellin. *Plant Physiol.* 108: 787–793.

Asano, T., Hayashi, N., Kobayashi, M., Aoki, N., Miyao, A. and Mitsuhara, I. (2012) A rice calcium-dependent protein kinase OsCPK12 oppositely modulates salt-stress tolerance and blast disease resistance. *Plant J.* 69: 26–36.

Asano, T., Kunieda, N., Omura, Y., Ibe, H., Kawasaki, T. and Takano, M. (2002) Rice SPK, a calmodulin-like domain protein kinase, is required for storage product accumulation during seed development. *Plant Cell* 14: 619–628.

Asano, T., Wakayama, M., Aoki, N., Komatsu, S., Ichikawa, H. and Hirochika, H. (2010) Overexpression of a calcium-dependent protein kinase gene enhance growth of rice under low-nitrogen conditions. *Plant Biotechnol.* 27: 369–373.

Berridge, M.J., Lipp, P. and Bootman, M.D. (2000) The versatility and universality of calcium signalling. *Nat. Rev. Mol. Cell Biol.* 1: 11–21.

Blume, B., Nürnberger, T., Nass, N. and Scheel, D. (2000) Receptor-mediated increase in cytoplasmic free calcium required for activation of pathogen defense in parsley. *Plant Cell* 12: 1425–1440.

Brauer, E.K., Rochon, A., Bi, Y.M., Bozzo, G.G., Rothstein, S.J. and Shelp, B.J. (2011) Reappraisal of nitrogen use efficiency in rice overexpressing glutamine synthetase1. *Physiol. Plant.* 141: 361–372.

Bundó, M. and Coca, M. (2016) Enhancing blast disease resistance by overexpression of the calcium-dependent protein kinase OsCPK4 in rice. *Plant Biotechnol. J.* 14: 1357–1367.

Bush, D.S. (1995) Calcium regulation in plant cells and its role in signaling. *Annu. Rev. Plant Physiol. Plant Mol. Biol.* 46: 95–122.

Campo, S., Baldrich, P., Messeguer, J., Lalanne, E., Coca, M. and San, S.B. (2014) Overexpression of a calcium-dependent protein kinase confers salt and drought tolerance in rice by preventing membrane lipid peroxidation. *Plant Physiol.* 165: 688–704.

Chaw, S.-M., Chun-Chieh Shih, A., Wang, D., Wu, Y.-W., Liu, S.-M. and Chou, T.-Y. (2008) The mitochondrial genome of the gymnosperm cycas taitungensis contains a novel family of short interspersed elements, bpu sequences, and abundant RNA editing sites. *Mol. Biol. Evol.* 25: 603–615.

Chen, S.H., Li, X.X., Liao, W.S., Wu, J.H. and Chan, L. (1990) RNA editing of apolipoprotein B mRNA. Sequence specificity determined by in vitro coupled transcription editing. *J. Biol. Chem.* 265: 6811–6816.

Chen, S., Tao, L., Zeng, L., Vega-Sanchez, M.E., Umemura, K. and Wang, G.L. (2006) A highly efficient transient protoplast system for analyzing defence gene expression and protein–protein interactions in rice. *Mol. Plant Pathol.* 7: 417–427.

Chung, H.J., Sehnke, P.C. and Ferl, R.J. (1999) The 14-3-3 proteins: cellular regulators of plant metabolism. *Trends Plant Sci.* 4: 367–371.

Defalco, T.A., Bender, K.W. and Snedden, W.A. (2010) Breaking the code: Ca2+ sensors in plant signalling. *Biochem. J.* 425: 27–40.

Estruch, J.J., Kadwell, S., Merlin, E. and Crossland, L. (1994) Cloning and characterization of a maize pollen-specific calcium-dependent calmodulin-independent protein kinase. *Proc. Natl. Acad. Sci. USA* 91: 8837–8841.

Fan, X., Jia, L., Li, Y., Smith, S.J., Miller, A.J. and Shen, Q. (2007) Comparing nitrate storage and remobilization in two rice cultivars that differ in their nitrogen use efficiency. *J. Exp. Bot.* 58: 1729–1740.

Fan, S.-C., Lin, C.-S., Hsu, P.-K., Lin, S.-H. and Tsay, Y.-F. (2009) The *Arabidopsis* nitrate transporter NRT1.7, expressed in phloem, is responsible for source-to-sink remobilization of nitrate. *Plant Cell* 21: 2750–2761.

Fellbrich, G., Blume, B., Brunner, F., Hirt, H., Kroj, T., Ligterink, W., et al. (2000) Phytophthora parasitica elicitor-induced reactions in cells of Petroselinum crispum. *Plant Cell Physiol.* 41: 692–701.

Grant, J.J. and Loake, G.J. (2000) Role of reactive oxygen intermediates and cognate redox signaling in disease resistance. *Plant Physiol.* 124: 21–30.

Gray, M.W. and Covello, P.S. (1993) RNA editing in plant mitochondria and chloroplasts. *FASEB J.* 7: 64–71.

Guo, S., Zhang, T., Xing, Y., Zhu, X., Sang, X.C., Ling, Y., et al. (2014) Identification and gene mapping of an early senescence leaf 4 mutant of rice. *Crop Sci.* 54: 2713–2723.

Harmon, A.C., Gribskov, M., Gubrium, E. and Harper, J.F. (2001) The CDPK superfamily of protein kinases. *New Phytol*. 151: 175–183.

Harmon, A.C., Gribskov, M. and Harper, J.F. (2000) CDPKs—a kinase for every Ca2+ signal? *Trends Plant Sci.* 5: 154–159.

Harper, J., Sussman, M., Schaller, G., Putnam-Evans, C., Charbonneau, H. and Harmon, A. (1991) A calcium-dependent protein kinase with a regulatory domain similar to calmodulin. *Science* 252: 951–954.

Hepler, P.K., Vidali, L. and Cheung, A.Y. (2001) Polarized cell growth in higher plants. *Annu. Rev. Cell Dev. Biol.* 17: 159–187.

Hrabak, E.M., Chan, C.W.M., Gribskov, M., Harper, J.F., Choi, J.H., Halford, N., et al. (2003) The *Arabidopsis* CDPK-SnRK superfamily of protein kinases. *Plant Physiol.* 132: 666–680.

Hu, B., Wang, W., Ou, S., Tang, J., Li, H. and Che, R. (2015) Variation in NRT1.1B contributes to nitrate-use divergence between rice subspecies. *Nat. Genet.* 47: 834–838.

Jiang, H., Li, M., Liang, N., Yan, H., Wei, Y., Xu, X., et al. (2007) Molecular cloning and function analysis of the stay green gene in rice. *Plant J.* 52: 197–209.

Johnson, C.H., Knight, M.R., Kondo, T., Masson, P., Sedbrook, J., Haley, A., et al. (1995) Circadian oscillations of cytosolic and chloroplastic free calcium in plants. *Science* 269: 1863–1865.

Knight, H. and Knight, M.R. (2001) Abiotic stress signalling pathways: specificity and cross-talk. *Trends Plant Sci.* 6: 262–267.

Kolukisaoglu, U., Weinl, S., Blazevic, D., Batistic, O. and Kudla, J. (2004) Calcium sensors and their interacting protein kinases: genomics of the *Arabidopsis* and rice CBL-CIPK signaling networks. *Plant Physiol*. 134: 43–58.

Kudla, J., Xu, Q., Harter, K., Gruissem, W. and Luan, S. (1999) Genes for calcineurin B-like proteins in *Arabidopsis* are differentially regulated by stress signals. *Proc. Natl. Acad. Sci. USA* 96: 4718–4723.

Ladha, J.K., Kirk, G.J.D., Bennett, J., Peng, S., Reddy, C.K., Reddy, P.M., et al. (1998) Opportunities for increased nitrogen-use efficiency from improved lowland rice germplasm. *Field Crops Res*. 56: 41–71.

Larsson, C.M., Larsson, M., Purves, J.V. and Clarkson, D.T. (1991) Translocation and cycling through roots of recently absorbed nitrogen and sulphur in wheat (Triticum aestivum) during vegetative and generative growth. *Physiol. Plant.* 82: 345–352.

Lee, R.H., Wang, C.H., Huang, L.T. and Chen, S.C.G. (2001) Leaf senescence in rice plants: cloning and characterization of senescence up-regulated genes. *J. Exp. Bot.* 52: 1117–1121.

Lim, P.O., Kim, H.J. and Hong, G.N. (2007) Leaf senescence. *Annu. Rev. Plant Biol.* 58: 115–136.

Liu, K.H., Niu, Y., Konishi, M., Wu, Y., Du, H., Sun, C.H., et al. (2017) Discovery of nitrate-CPK-NLP signalling in central nutrient-growth networks. *Nature* 545: 311–316.

Luan, S., Kudla, J., Rodriguez-Concepcion, M., Yalovsky, S. and Gruissem, W. (2002) Calmodulins and calcineurin B-like proteins: calcium sensors for specific signal response coupling in plants. *Plant Cell* 14: S389–S400.

Ma, X., Cheng, Z., Qin, R., Qiu, Y., Heng, Y., Yang, H., et al. (2013) OsARG encodes an arginase that plays critical roles in panicle development and grain production in rice. *Plant J.* 73: 190–200.

Marschner, H. (2012) Marschner's Mineral Nutrition of Higher Plants. Academic Press, London.

Mower, J.P. (2005) PREP-Mt: predictive RNA editor for plant mitochondrial genes. *BMC Bioinformatics.* 6: 96–110.

Oliveira, I.C., Brears, T., Knight, T.J., Clark, A. and Coruzzi, G.M. (2002) Overexpression of cytosolic glutamine synthetase. Relation to nitrogen, light, and photorespiration. *Plant Physiol*. 129: 1170–1180.

Park, S.Y., Yu, J.W., Park, J.S., Li, J., Yoo, S.C., Lee, N.Y., et al. (2007) The senescence-induced staygreen protein regulates chlorophyll degradation. *Plant Cell* 19: 1649–1664.

Petschek, J.P., Mermer, M.J., Scheckelhoff, M.R., Simone, A.A. and Vaughn, J.C. (1996) RNA editing in Drosophila 4f-rnp gene nuclear transcripts by multiple A-to-G conversions. *J. Mol. Biol.* 259: 885–890.

Roberts, D.M. and Harmon, A.C. (1992) Calcium-modulated proteins: targets of intracellular calcium signals in higher plants. *Annu. Rev. Plant Physiol. Plant Mol. Biol.* 43: 375–414.

Romeis, T., Ludwig, A.A., Martin, R. and Jones, J.D.G. (2001) Calcium-dependent protein kinases play an essential role in a plant defence response. *EMBO J.* 20: 5556–5567.

Romeis, T., Piedras, P. and Jones, J.D. (2000) Resistance gene-dependent activation of a calcium-dependent protein kinase in the plant defense response. *Plant Cell* 12: 803–815.

Saijo, Y., Hata, S., Kyozuka, J., Shimamoto, K. and Izui, K. (2000) Overexpression of a single Ca2+-dependent protein kinase confers both cold and salt/drought tolerance on rice plants. *Plant J.* 23: 319–327.

Sanders, D., Brownlee, C. and Harper, J.F. (1999) Communicating with calcium. *Plant Cell* 11: 691–706.

Sang, X., Li, Y., Luo, Z., Ren, D., Fang, L., Wang, N., et al. (2012) CHIMERIC FLORAL ORGANS 1, encoding a monocot-specific MADS box protein, regulates floral organ identity in rice. *Plant Physiol*. 160: 788–807.

Sato, Y., Morita, R., Katsuma, S., Nishimura, M., Tanaka, A. and Kusaba, M. (2009) Two short-chain dehydrogenase/reductases, NON-YELLOW COLORING 1 and NYC1-LIKE, are required for chlorophyll b and light-harvesting complexII degradation during senescence in rice. *Plant J.* 57: 120–131.

Sheen, J. (1996) Ca2+-dependent protein kinases and stress signal transduction in plants. *Science* 274: 1900–1902.

Snedden, W.A. and Fromm, H. (1998) Calmodulin, calmodulin-related proteins and plant responses to the environment. *Trends Plant Sci.* 3: 299–304.

Tamura, K., Stecher, G., Peterson, D., Filipski, A. and Kumar, S. (2013) MEGA6: molecular evolutionary genetics analysis version 6.0. *Mol. Biol. Evol.* 30: 2725–2729.

Toroser, D. and Huber, S.C. (1997) Protein phosphorylation as a mechanism for osmotic-stress activation of sucrose-phosphate synthase in spinach leaves. *Plant Physiol.* 114: 947–955.

Trewavas, A. (1999) How plants learn. *Proc. Natl. Acad. Sci. USA* 96: 4216–4218.

Trewavas, A.J. and Malhó, R. (1998) Ca2+ signalling in plant cells: the big network! *Curr. Opin. Plant Biol.* 1: 428–433.

Wang, L., Kimble, J. and Wickens, M. (2004) Tissue-specific modification of gld-2 mRNA in C. elegans: likely C-to-U editing. *RNA* 10: 1444–1448.

Wang, J., Li, G. and Kai, X. (2007) Characterization and expression analysis of calcium-dependent protein kinase genes in rice(*Oryza sativa L.*). *Front. Agric. China* 1: 397–404.

Wei, S., Hu, W., Deng, X., Zhang, Y., Liu, X., Zhao, X., et al. (2014) A rice calcium-dependent protein kinase OsCPK9 positively regulates drought stress tolerance and spikelet fertility. *BMC Plant Biol.* 14: 133–145.

Xu, H. and Heath, M.C. (1998) Role of calcium in signal transduction during the hypersensitive response caused by basidiospore-derived infection of the cowpea rust fungus. *Plant Cell* 10: 585–597.

Yamaya, T., Obara, M., Nakajima, H., Sasaki, S., Hayakawa, T. and Sato, T. (2002) Genetic manipulation and quantitative-trait loci mapping for nitrogen recycling in rice. *J. Exp. Bot.* 53: 917–925.

Yang, G.X. and Komatsu, S. (2000) Involvement of calcium-dependent protein kinase in rice (*Oryza sativa L.*) lamina inclination caused by brassinolide. *Plant Cell Physiol*. 41: 1243–1250.

Yang, Y., Lv, J., Gui, B., Yin, H., Wu, X., Zhang, Y., et al. (2008) A-to-I RNA editing alters less-conserved residues of highly conserved coding regions: implications for dual functions in evolution. *RNA* 14: 1516–1525.

Zhou, Y., Huang, W., Liu, L., Chen, T., Zhou, F. and Lin, Y. (2013) Identification and functional characterization of a rice NAC gene involved in the regulation of leaf senescence. *BMC Plant Biol.* 13: 132–144.

Zhu, S.Y., Yu, X.C., Wang, X.J., Zhao, R., Li, Y., Fan, R.C., et al. (2007) Two calcium-dependent protein kinases, CPK4 and CPK11, regulate abscisic acid signal transduction in Arabidopsis. *Plant Cell* 19: 3019–3036.

Zielinski, R.E. (1998) Calmodulin and calmodulin-binding proteins in plants. *Annu. Rev. Plant Physiol. Plant Mol. Biol.* 49: 697–725.